Spectrochimica Acta Part A: Molecular and Biomolecular Spectroscopy 267 (2022) 120546

Contents lists available at ScienceDirect

Spectrochimica Acta Part A: Molecular and Biomolecular Spectroscopy

journal homepage: www.elsevier.com/locate/saa

Photophysical properties and bioimaging application of an aminonaphthalimide-squaraine non-conjugated system

Vladimir Stamentović [a], Daniel Collado [a,b,*], Ezequiel Perez-Inestrosa [a,b,*]

[a] Universidad de Málaga-IBIMA, Departamento de Química Orgánica, Campus de Teatinos s/n, 29071 Málaga, Spain
[b] Centro Andaluz de Nanomedicina y Biotecnología–BIONAND, Parque Tecnológico de Andalucía, C/ Severo Ochoa 35, 29590 Campanillas, Málaga, Spain

HIGHLIGHTS

- New red emissive aminonaphthalimide-squaraine non-conjugated.
- Ratio of the two emissions (I_{SQ}/I_{naph}) depend on the polarity of the medium.
- TPA absorption of 1 gives intense fluorescent response signal in microscopy images.

GRAPHICAL ABSTRACT

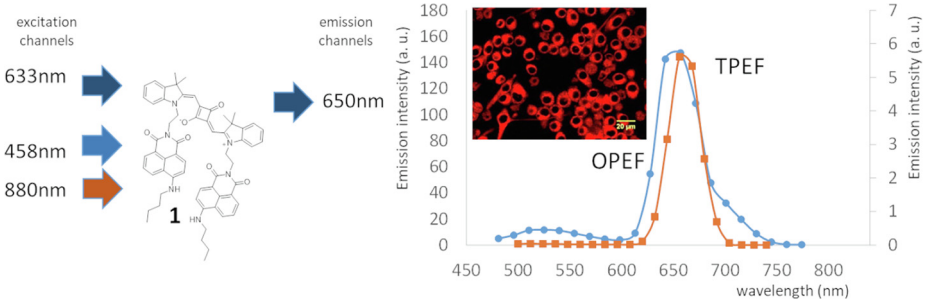

ARTICLE INFO

Article history:
Received 8 August 2021
Received in revised form 23 October 2021
Accepted 24 October 2021
Available online 28 October 2021

Keywords:
Squaraine
Naphthalimide
Energy Transfer
Two-photon absorption
Cell bioimaging

ABSTRACT

An aminonaphthalimide-squaraine non-conjugated system was designed and synthetized with the purpose of preparing fluorescent molecule in the 650–700 nm region that could operate via energy transfer (ET) between covalently linked naphthalimide and squaraine chromophores. The photophysical properties of the new fluorescent system were explored with the aim of understanding the ET in one- and two-photon excitation modes. The spectroscopic techniques employed in the characterization includes; absorption, fluorescence, quantum yields and fluorescence lifetime measurements in different solvents. The effect of polarity of solvents on efficiencies of ET were evaluated using one- and two-photon excited fluorescence. The optical behavior of the non-conjugated system was compared with its individual squaraine and naphthalimide moieties. The two-photon absorption (TPA) spectrum of the molecule was obtained between 750 and 1040 nm, with the largest two-photon cross section (δ_{TPA})above 4200 GM. Finally, the applicability of the molecule for fluorescence imaging in the one- and two-photon excitation mode was demonstrated in N13 Microglial cells. The *in vitro* and *in vivo* confocal microscopy studies indicated that the non-conjugated system efficiently accumulated in the cytoplasm suggesting it could be utilized as a subcellular probe.

1. Introduction

One of the leading mechanisms and widely used in labelling biological molecules is the electronic energy transfer (ET). It often plays a crucial role in the design of fluorescence probes [1]. ET is also used as a single-molecule technique for measuring distances within and between molecules.[2] Based on through-space energy transfer, the spectra overlap in between the donor (D) emission

* Corresponding authors at: Universidad de Málaga-IBIMA, Departamento de Química Orgánica, Campus de Teatinos s/n, 29071 Málaga, Spain.
E-mail addresses: dcollado@uma.es (D. Collado), inestrosa@uma.es (E. Perez-Inestrosa).

https://doi.org/10.1016/j.saa.2021.120546
1386-1425/

and the acceptor (A) absorption in a period of ET systems has been used successfully to artificially enhance the Stokes shift of an energy transfer cassette.[3] This pseudo-Stokes shift is relevant in fluorophore with small difference between positions of the band maxima of the absorption and emission spectra. Small Stokes shifts of a dye can cause re-excitation that affect its detection sensitivity, which is a potential drawback for their application in bioimaging.[4] This problem could be overcome in excitation energy transfer (EET) systems that absorb at short wavelength and emit efficiently at much longer wavelengths, and might therefore be useful in applications that requires several dyes in a multiplexed biochemical experiment.[5] This type of synthetic approach to obtain EET systems have been applied to BODIPY fluorophores which are molecules with strong absorption and emission. However, this fluorophore display small difference between absorption and emission maxima (10–25 nm). For example, an ET based naphthalimide-BODIPY dyad has been elaborated by merging a naphthalimide fluorophore to a BODIPY.[6] The ET cassettes were found to display very fast and efficient aminonaphthalimide-BODIPY fluorescence sensitization. This was detected by one- and two-photon excitation, which enhances the application range of the investigated bichromophoric dyad in terms of accessible excitation wavelengths. Contrarily, squaraine's strong absorption (ϵ > 200000 mol^{-1} cm^{-1}) and fluorescence emission make it an ideal candidate for harvesting/emitting photons in the near-infrared (NIR) region which reduces the overlap with the fluorescence emission of any biomolecule in bioimaging applications.[7,8] However, the squaraine Stokes shift are usually small (10–20 nm) and some effort have been made to increase the shift between emission signals and the excitation wavelength.[9] In this way, ET systems that improve the optical properties of squaraines can have practical application in bioimaging.

Two-photon excited fluorescence plays an important role in more recent bioimaging technics. It use longer excitation wavelength to visualize samples that improves its imaging depths and provides valuable biological information inside the sample.[10] In comparison to one-photon excited fluorescence (OPEF), TPEF offers several advantages, such as high spatial resolution, deep tissue penetration, and low background noise compare with traditional OPEF imaging.[11]

Recently, researches have shown interest in the TPEF properties of squaraines, as a result of their electron-withdrawing character strength and display intramolecular charge transfer when adhered to groups of electron donor, in addition to significant two-photon absorption (TPA) properties.[12]

Herein, we characterize the OPEF and TPEF properties of a new naphthalimide-squaraine non-conjugated system **1**. This molecule consists of a non-conjugated D/A energy system where the donor dye is 4-aminonaphthalimide and the acceptor dye an indolic squaraine derivative (scheme 1). Naphthalimide is one of the most applied fluorophores in dyes design for its simple chemical modification, prominent photostability, emission in the visible range and large Stokes shift.[13] Indolenine-based squaraines are more attractive for the design of fluorescent labels and probes due to their higher photostability compared to similar cyanines and other aromatic squaraines.[14] Whaťs more, both fluorophores possess good brightness, stability and insensitivity to the pH of the environment.

Squaraine exhibits bright OPEF and TPEF in organic solvents and can be complemented in water when adding bovine or human serum albumin.[15] In presence of the protein, the two-photon properties of squaraine increased by 200 times compared to the individual squaraine. Benzoindolic squaraine dyes with different benzyl groups in non-conjugated Donor/Acceptor (D/A) energy systems show a large two-photon absorption cross-section above 12,000 GM (1 GM = 1 × 10^{-50} cm^4 s/photon).[16] It is acknowledged that for deep tissue bioimaging, it would be convenient that the squaraine dye with intense NIR emission, favorable photostability and low biotoxicity. Molecule **1** combine the photophysical characteristics for an appropriate candidate for the study of the effect of biological condition in cells in the process of energy transfer. The synthesis of **1** was carried out by a conventional synthesis of squarylium dyes by condensation of 3,4-dihydroxy-3-cyclobutene-1,2-dione (squaric acid) with two equivalents of indolinium salts that contain the energy donor unit. This synthesis allows to obtain a multichromophoric triad with two energy donor units per energy acceptor. This configuration maximize the absorption of energy by the donor unit and favor the ET process to acceptor unit (antenna effect). The photophysical properties of **1** were compared with the reference compounds **2** and **3**.

2. Materials and methods

2.1. Synthesis of compounds *1*

The synthetic routes are shown in Scheme 2. The squaraine reference compound **2** was obtained according to the previous procedure.[12,17] Compound **3** was synthetized from 4-bromo-1,8-naphthalic anhydride.[19] The synthesis and characterization of new compound **1** can be found in the Supporting Information.

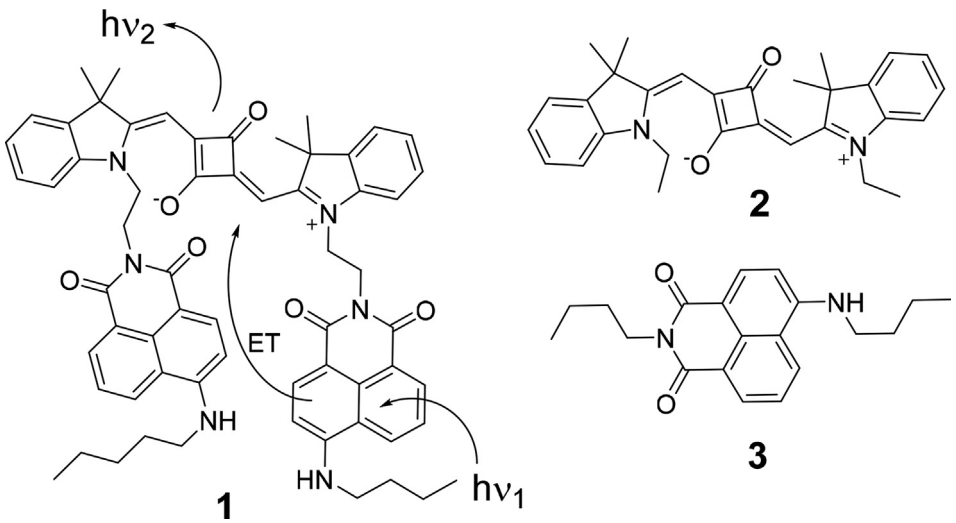

Scheme 1. Structures of molecule **1** and reference compounds **2** and **3**.

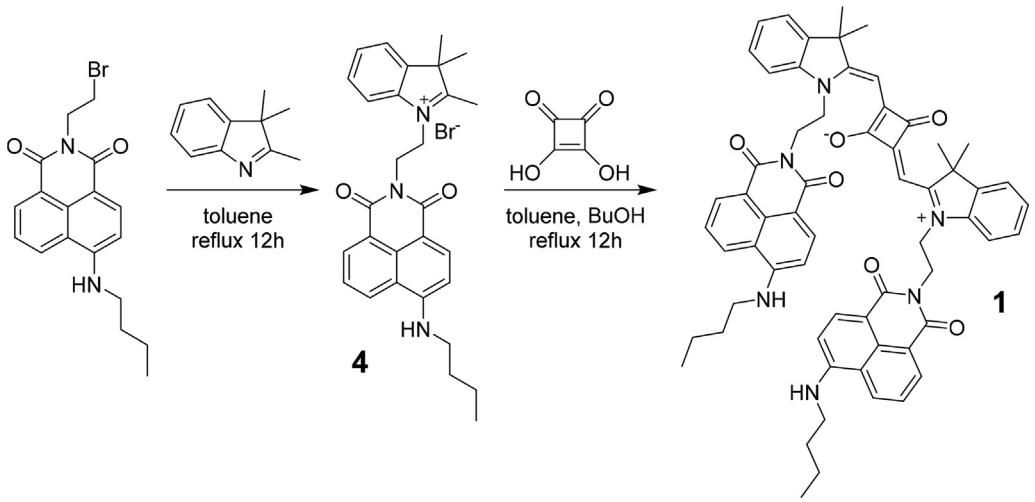

Scheme 2. Synthesis route of **1**.

2.2. Photophysical characterization

Absorption measurements were performed on a Varian CARY 100 Bio UV–vis spectrophotometer and fluorescence measurements on an Edinburgh Instruments FLS920 spectrofluorometer. Fluorescence decay curves were measured in different solvents using an Edinburgh Instruments FLS920 time-correlated single-photon counting system. Two light emitting diodes Picoquant PLS-Series at 450 and 650 nm were used for excitation. The TPA cross sections (δ) were determined by the two-photon-induced-fluorescence method [20] between 700 and 1000 nm in a Leica SP5 AOBS MP instrument, equipped with a MaiTai Ti:Sapphire HP laser (Spectra-Physics, Inc.) tunable between 690 and 1040 nm. Confocal and Multiphoton Microscopy of Fluorophores in Biological Conditions was carried out in same equipment as used for the fluorophores alone. Under OPEF conditions, confocal excitation lasers (458 and 633 nm) were used. Two-photon emission spectra were obtained for 880 nm excitation. See Supporting Information for more detailed methods. Spectroscopic measurements were conducted in solvents of different polarity: toluene (TOL); tetrahydrofuran (THF); dimethylformamide (DMF); methanol (MeOH); ethanol (EtOH); *n*-propanol; *n*-pentanol; *n*-hexanol; *n*-octanol; *n*-decanol; acetonitrile (CH_3CN); chloroform ($CHCl_3$) at room temperature.

3. Results and discussion

3.1. Synthesis

The synthesis of triad **1** was completed in two steps, as shown in Scheme 2. Naphthalimide-indolium **4** was synthetized by condensation of commercially available indolenine and naphthalimide derivative in toluene under reflux in a sealed tube. Subsequently, by condensation of squaric acid with **4** in n-butanol/toluene mixture and under azeotropic distillation conditions, the squaraine dye **1** was achieved.[21] The symmetrical squaraine **2** and naphthalimide **3** were prepared and applied as model compounds in comparison to photophysical properties with the compound **1**. The purity and characterization of synthetized compounds were carried out by NMR, HRMS, linear and nonlinear spectroscopic studies.

3.1.1. Linear absorption and fluorescence spectra

In molecule **1** is expected that naphthalimide acts as an energy donor and squaraine as an energy acceptor. The efficiency of ET is mainly determine by the distance between the two fluorophores and the overlap between the donor's emission and the acceptor's absorption bands. In the design of non-conjugated system **1** as an energy donor, naphthalimide fluorophore was appointed due to the strong emission in the visible range and its broad emission (450–650 nm) which covers a part of squaraine absorption band (550–670 nm) indicating the possibility of ET. The absorption spectra of **1** showed the characteristic bands of naphthalimide and squaraine. As displayed in Fig. 1.a, the absorption bands at 437 nm (ε = 28595 M^{-1} cm^{-1}) and 639 nm (ε = 202353 M^{-1} cm^{-1}) in CH_3CN certainly demonstrated the presence of naphthalimide and squaraine within **1**. The comparison of the absorption bands of **1** with reference compounds **2** and **3** clearly indicates that the absorption band with maximum at 639 nm corresponds to squaraine while the second band at 437 nm corresponds to naphthalimide (Fig. 1.b). Since the absorption spectrum of **1** agrees with the sum of the spectra of the corresponding energy acceptor and donor and the formation of new bands is not observed, there is no evidence of electronic interaction between the acceptor and donor chromophores in the triad.

The energy transfer process was activated upon excitation of naphthalimide subchromophore in **1** at 430 nm. Two emission bands were observed with maximum at 525 nm and at 659 nm (in CH_3CN) correspond to emission of naphthalimide and squaraine, respectively (Fig. 1). The presence of these two bands simultaneously in the emission spectrum of **1** indicates that the ability of energy transfer would be big but not complete.

Excitation of **3** at 430 nm resulted in CH_3CN an intense and broad emission at 528 nm; however, in triad **1** at the same excitation wavelength, the intensity corresponding to the donor emission was quenched by 92% compared to the reference molecule **3**. At the same time, the intensity corresponding to the acceptor at 652 nm increased by>20000-fold compared to direct excitation of reference molecule **2** at 430 nm (Fig. 2.a). The energy transfer process in triad **1** was also confirmed by excitation spectrum at λ_{em} = 655 nm. The absorption bands of both the constituent subchromophores observed in the spectrum suggesting efficient energy transfer from donor to acceptor energy (Fig. 2.b). It should be noted that in both absorption and emission spectrum of **1**, the bands are clearly assignable and no new bands appear associated with charge transfer phenomena.

3.1.2. Effect of solvent polarity

Squaraines due to the polar nature of their structure have been used as environment-sensitive dyes, which change their intensity

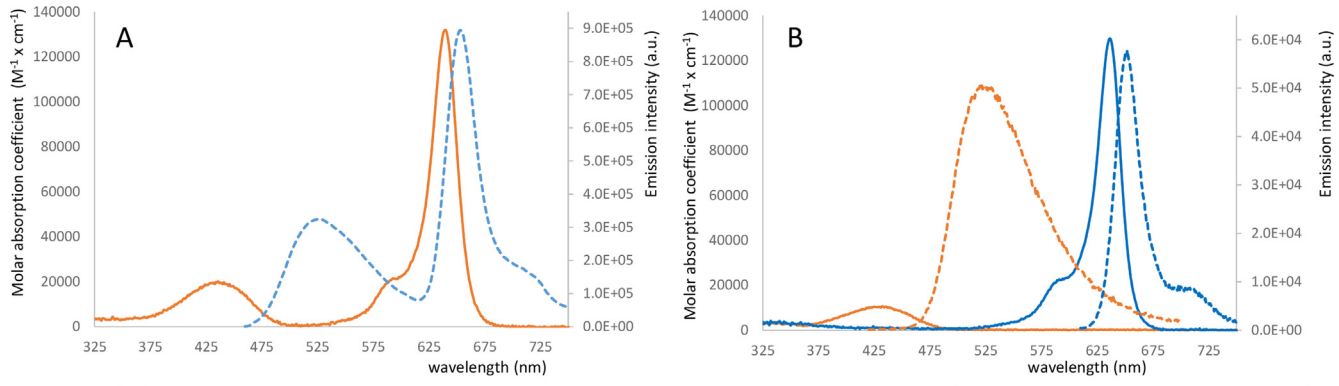

Fig. 1. A) UV/Vis absorption (solid lines) and fluorescence spectra (dashed lines, λ_{exc} = 430 nm) of **1** in CH_3CN. B) UV/Vis absorption (solid lines) and fluorescence spectra (dashed lines, λ_{exc} = 430 nm) of the models **2** (blue) and **3** (orange) in CH_3CN.

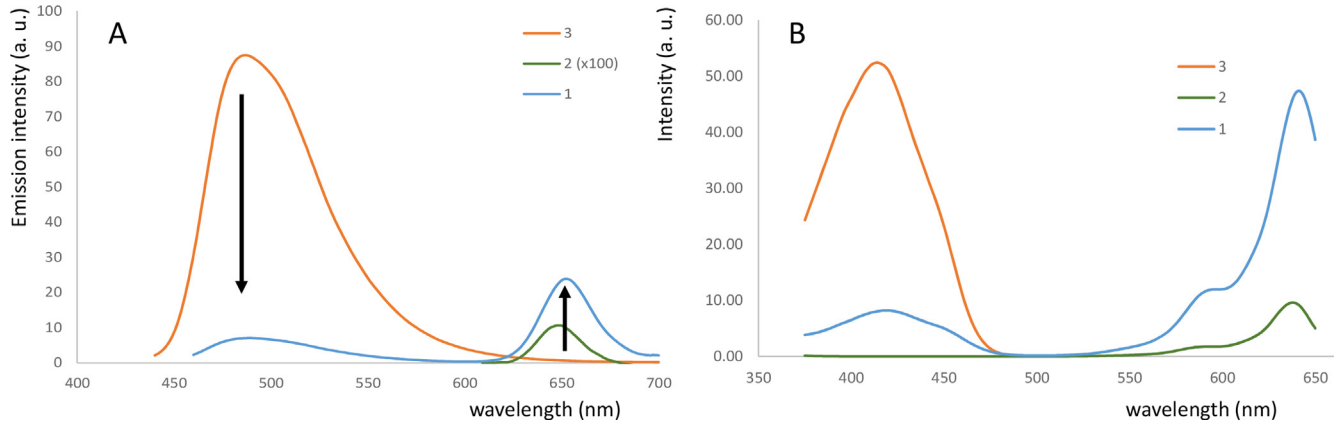

Fig. 2. A) Fluorescence spectra of **1**, **2** and **3**, in TOL (λ_{exc} = 430 nm, c ≈ 7 × 10^{-6} M). B) Fluorescence excitation spectra of **1**, **2** and **3** in TOL (λ_{em} = 655 nm).

as a function of solvent polarity and/or viscosity.[22] In particular, indole-based squaraines exhibits fluorescence enhancement in apolar media combined with high photostability. Solvent-dependent absorption and emission properties of several substituted squaraines have been observed, leading to the proposal of a solute–solvent strong interaction in the ground and excited state.[23] We studied the photophysical behavior of triad **1** in solvents of diverse polarity including polar to non-polar and protic to aprotic solvents. As it is seen on the data displayed on Table 1, the spectroscopic properties of **1** depend on the polarity of solvent used. The maxima of the absorption of **1** in different solvents (TOL, THF, CH_3CN, $CHCl_3$, DMF, and MeOH) were in the range 426–449 nm for 4-aminonaphthalimide moiety and 637–643 nm for squaraine moiety (Fig. 3.a). For fluorescence emission, the maxima were observed in the range of 493–541 nm and 648–654 nm for the naphthalimide and squaraine subchromophore respectively.

An increase of solvent polarity results in a blue shift of absorption spectra for squaraine and red shift of absorption band for 4-aminonaphthalimide. These exhibited negative and positive solvatochromism (for squaraine and naphthalimide, respectively) are known spectral characteristics of these fluorophores.[24,25] The negative and positive solvatochromism are observed also in the emission spectra (Table 1). The resulting effect is that the squaraine absorption bands and the naphthalimide emission band are closer together as the polarity of the solvent increases. The emission maxima of the triad **1** showed weak blue-shift (6 nm) upon increasing solvent polarity from TOL to methanol in line with previous reports.[26,27] This change is small to be considered in an

Table 1
Effect of solvents in the photophysical data of **1**.

Solvent		Naphthalimide subchromophore			Squaraine subchromophore						
	ET(30)[(5)]	$\lambda_{ab\ max}$	log (ε)	$\lambda_{em\ max}$	$\lambda_{ab\ max}$	log (ε)	$\lambda_{em\ max}$	$\Delta\lambda_{ab}$[(1)]	Φ_F[(2)]	I_{SQ}/I_{naph}[(3)]	$\Delta\lambda_{em}$[(4)]
TOL	33.9	426	4.30	493	643	5.33	654	217	41	14.9	161
THF	37.4	431	4.35	503	642	5.36	653	211	40	11.2	150
$CHCl_3$	39.1	433	4.55	504	641	5.44	652	208	24	8.2	148
DMF	43.2	435	4.34	519	640	5.20	650	205	23	6.1	131
CH_3CN	45.7	437	4.46	529	639	5.31	649	202	12	2.4	129
MeOH	55.4	449	4.45	541	637	5.28	648	188	7	2.0	107

(1) difference between naphthalimide-squaraine absorption maxima (in nm), (2) total quantum yield (%), (3) relation intensities of the emission bands λ_{exc} = 430 nm, (4) difference between naphthalimide-squaraine emission maxima (in nm), (5) empirical solvatochromic solvent polarity parameter.

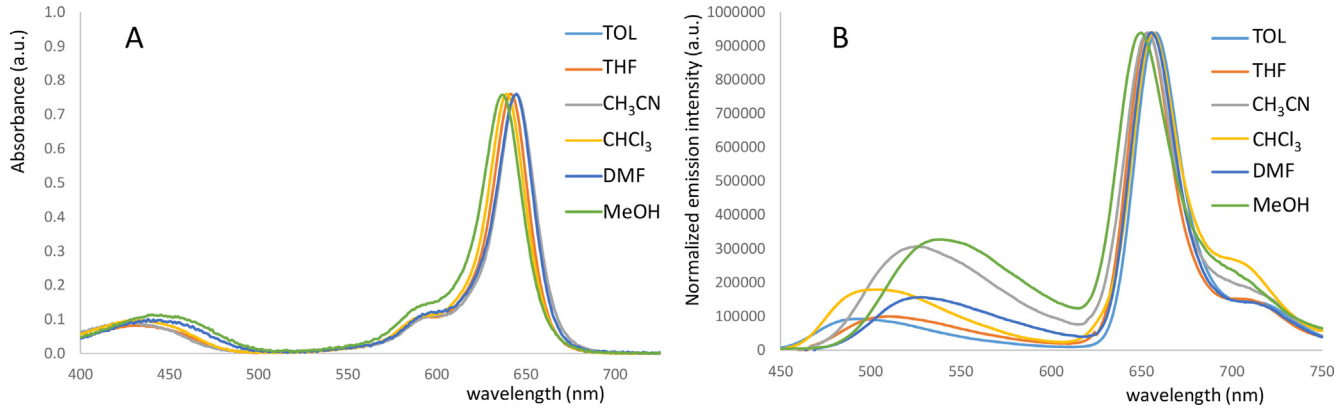

Fig. 3. A) UV − vis absorbance spectra of **1** in some organic solvents. B) Emission spectra of **1** in some organic solvents (λ_{exc} = 430 nm).

environmental-sensitive fluorophore. More interesting is to consider the effect of solvent polarity on the ratio of emission intensities of fluorophores (I_{SQ}/I_{naph}) in molecule **1** at 430 nm excitation wavelength. The I_{SQ}/I_{naph} ratio is related to the efficiency in the ET between both fluorophores. Good linear connections of maximum absorption peaks with solvent polarity parameters (Bayliss, Lorentz–Lorenz or ET(30) polarity scales) have been reported previously for several squaraines.[19,28] This parameter is widely used as a parameter of linear solvation energy relationships for the correlation analysis of solvent effects on physical and chemical properties.[29] Spectral positions of the fluorescence emission of **1** exhibit the same strong dependence on solvent polarity (Figure S1) using the empirical solvatochromic solvent polarity parameter ET (30). The higher the value of this ratio, the better the transfer of energy between naphthalimide and squaraine is to be expected. The value of this ratio clearly decreases as the polarity of the solvent increases, from 14.9 in toluene to 2.0 in methanol. This variation of the I_{SQ}/I_{naph} value of is in good relation with the value of the empirical parameter ET(30) with correlation coefficient higher than 0.97. It is knows that the ET(30) values do not provide good correlations in hydrogen-bond donor solvent. In methanol, the I_{SQ}/I_{naph} value is higher than expected (Figure S1), which indicates the influence of hydrogen bonds on the stability of the molecule.

Additional studies were made to examine the effect of solvent polarity on fluorescence emission for **1** at 25 °C, and the results are given in Table S1 and Figure S2. The solvents used were a series of alkanols with different unbranched saturated chain of carbon atoms.[30] Throughout this set of solvents, both absorption and emission maxima show a dependence on the polarizability of the medium. More significantly, I_{SQ}/I_{naph} values decreases progressively with increasing ET(30) is in good correlation with the polarity of the solvent (Figure S1). This indicates that the ratio I_{SQ}/I_{naph} could be a good parameter to determine the polarity of the environment around triad **1**. The dependence of fluorescence emission with polarity is clearly observed in fluorescence quantum yields (Φ_F) which decreased systematically with the increase in solvent polarity from TOL to methanol (Table 1) and from decanol to methanol (Table S1). The quantum yields of triad **1** were compared with reference molecules **2** and **3**. A decrease in the emission of the energy donor quantum yield at 500 nm is observed in the triad (≈8%) compared with molecule **3** in TOL. In this solvent, the efficiency of energy transfer (EET) can be estimated to be 91% (Table S2). This value, although high, does not allow the complete quenching of the fluorescence intensity of naphthalimide but ensured the double-wavelength emissions in **1**. EET was also calculated in CH_3CN and MeOH giving similar values (Table S2).

We examined the emission behavior of **1** in MeOH/H_2O mixtures because **1** is soluble in MeOH, but less soluble in water, and it would aggregate in MeOH/H_2O mixtures with a high water fraction (f_w). In MeOH/H_2O mixtures, only a slight bathochromic shift is observed in the absorption spectra as the f_w increases. The emission from squaraine moiety of **1** in MeOH/H_2O (f_w = 20) solution show a large decrease (49% in emission area compared with pure MeOH). It has been observed in previous squaraines studies in dioxane:water mixtures that water addition produces a drastic increase of nonradiative processes. [31] This fluorescence emission reduction effect is less visible in naphthalimide since the naphthalimide band remains unchanged at 540 nm (Figure S3). The general effect in **1** is the decrease in value of I_{SQ}/I_{naph} ratio in a good linearity range between 0 and 20% of water. At f_w values>20, the fluorescence emission from squaraine at λ_{exc} = 430 nm is quenched and only emission from naphthalimide is detected in H_2O (Figure S4). In pure water, the absorption band of squaraine subchromophore was blue shifted and broadened with decrease in the extinction coefficient, indicating the formation of H-aggregates. It is well known that in polar solvents squaraine dyes are prone to the formation of aggregate assemblies due to intermolecularπ−πand hydrophobic interactions.[32] The formation of aggregates were confirmed by DLS experiment in MeOH/H_2O mixtures. At f_w = 80%, the formation of 65.5 ± 3.8 nm diameter aggregates is observed with a polydispersity index of 0.06 (Figure S5). Molecule **1** showed a clear environment-sensitive fluorescence enhancement from water to apolar TOL (Table S1). This property is attractive in cellular imaging because it reduces background emission from the fluorescent probe.[33]

3.1.3. Fluorescence lifetimes

Table 2 shows the experimental lifetimes in different solvents. Fluorescence decay curves for compound **1** are reported in Figure S6. Compound **1** showed a mono exponential decay (τ_1) at 650 nm (emission from squaraine) in apolar solvents like TOL or THF. In more polar solvents, the fluorescence decay is biexponential with a small contribution (∼6%) of the second (longer) compo-

Table 2
Measured Lifetimes for **1** in some solvents (λ_{exc} = 450 nm, λ_{em} = 650 nm).

Solvent	*ET(30)*[(1)]	τ_1 (ns)[(2)]	τ_2 (ns)[(2)]	χ^2
TOL	33.9	1.9 (100)	–	1.333
THF	37.4	1.4 (100)	–	1.401
$CHCl_3$	39.1	1.1 (96)	3.5 (4)	1.110
DMF	43.2	0.9 (93)	6.6 (7)	1.498
CH_3CN	45.7	0.4 (98)	8.5 (3)	1.111
MeOH	55.4	0.2 (95)	7.0 (5)	1.188

[(1)] empirical solvatochromic solvent polarity parameter; [(2)] amplitudes of the components for double-exponential decay are shown in parentheses.

nent τ_2 (Table 2). This effect is more evident in a series of linear *n*-alkanols (from methanol to decanol) where there is an increase in the lifetime together with a decrease in the polarity of the solvent expressed in terms of solvent polarity parameter ET(30) (Table S3 and Figure S7). The second long-lived component of the fluorescence emission presumably can be explained by emissive species specifically solvated in more polar solvents.[18] Specifically, the fluorescence intensity decay times for **1** increased from τ_1 = 0.2 ns in methanol to τ_1 = 2.2 ns in decanol. The increase in the lifetime observed is parallel with an increase in the fluorescence quantum yield of **1**. However, lifetime values are similar to those observed for chromophore **2** (Table S4), which show typical single-exponential character.

A lifetime analysis of reference compound **3** and triad **1** allow quantify the EET.[34] Compound **1** showed a bi-exponential decay (τ_1 and τ_2) at 520 nm (emission from naphthalimide) with an average fluorescence lifetime (4.0, 5.1 and 4.7 ns in TOL, CH_3CN and MeOH) lower than the reference compound **3** (9.8, 10.2 and 9.2 ns in TOL, CH_3CN and MeOH). Consequently, EETs were calculated to be ≈60% in TOL, 56% in CH_3CN and 48% in MeOH for triad **1** (Table S4).

3.1.4. Fluorescence spectra in the presence of BSA

Previous studies using several squaraine dyes showed considerably higher emission in the presence of bovine serum albumin (BSA) or human serum albumin (HSA) and were used for the determination of proteins.[35] In particular, the fluorescence emission of molecule **2** in water was enhanced 17.7 times by adding BSA in the solution. [36] We examined the interaction of triad **1** with BSA. The fluorescence spectra of triad **1** at different concentration of BSA are shown in Fig. 4. No increase in the emission intensity of the squaraine subchromophore is observed, indicating that there is no interaction between this part of the molecule and the protein. However, a modest increase in the fluorescence emission (2.7-fold) of the naphthalimide subchromophore is shown. This observation confirms the dye ability to interact with the BSA. This noncovalent interactions have previously been described to involve hydrophobic, electrostatic and hydrogen bonding interactions.[37] The hypsochromic shift of the emission band shown in Fig. 7.b is in agreement with a hydrophobic interaction between the naphthalimide and the protein.

3.1.5. Effect temperature in the fluorescence spectra

Molecules that exhibit dual fluorescence can be used in analyte sensing or temperature monitoring. They have the advantages that they operate independently of the light intensity used and allow self-calibration.[38] We examined the effect of temperature on the ET process in triad 1. Variable temperature experiments were performed in butironitrile because of the wide temperature range available. The emission of naphthalimide subchromophore at 550 nm for triad **1** did not change significantly with temperature while emission at 655 nm changed significantly (Fig. 5.a). The analysis of the I_{SQ}/I_{naph} ratio as a function of temperature showed a linear fitting with a high degree of correlation (R^2 = 0.969). The slope of the fitted curve give negative coefficient as squaraine fluorescence emission decreases with temperature.[39] From this slope, it can be determined that the thermal sensitivity shown by triad **1** has a value of 0.26 % K^{-1} in the temperature range of 110–360 K. To the best of our knowledge, this is the first report of temperature sensing for a squaraine-containing triad.

3.2. Two-Photon absorption (TPA) properties

The development of new organic materials for two-photon absorption (TPA) is an area of continuous research with practical applications in bioimaging. Molecules with a large TPA cross section can use longer excitation wavelength that improves its imaging depths, which gives deeper biological information.[40] Some of the common problems for tissue and cellular imaging, light scattering, absorption and auto-fluorescence diminish substantially when the samples are stimulated with longer wavelength light. As the same time, the excitation mode with IR o NIR light compared to visible and UV light has been proven to induce less damage to the samples. So significant photoluminescence properties in the NIR and high δ_{TPA} values are optical characteristic to be considered in an efficient probe for two-photon fluorescence bioimaging. However, compared with the large amount of OPEF dyes, the number of dyes with bright TPEF is relatively lower. A general methodology to obtain dyes with bright TPEF is the synthesis of extended π-conjugated frameworks and addition of donor and acceptor groups.[41] The donor–acceptor–donor (D–A–D) nature of the squaraine derivatives appeared very promising for two photon absorption processes at NIR range.[42] Squaraine dyes which are chained with π-conjugated frameworks, show bright TPEF and have been used for bioimaging.[43] The photophysical properties of compound **1** under TPE conditions and its effect on energy transfer process between naphthalimide and squaraine units was studied in several solvents.

The degenerate TPA spectra of **1, 2** and **3** were measured by TPEF method in the range 740–1000 nm and are shown in Fig. 6. In particular, the TPA spectrum of **1** was measured in various solvents (Figure S8). The nature of the TPA bands for **2** has been pre-

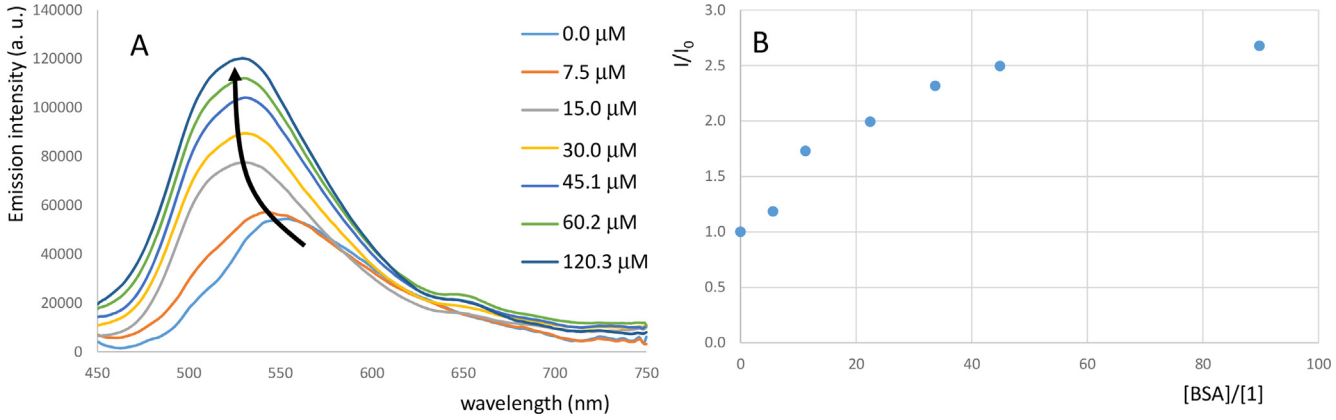

Fig. 4. A) Fluorescence spectra of **1** in PBS buffer pH = 7.24, with increasing concentrations of BSA (λ_{exc} = 440 nm). B) Fluorescence ratio (I/I_0) at 530 nm at different BSA/**1 M** ratio.

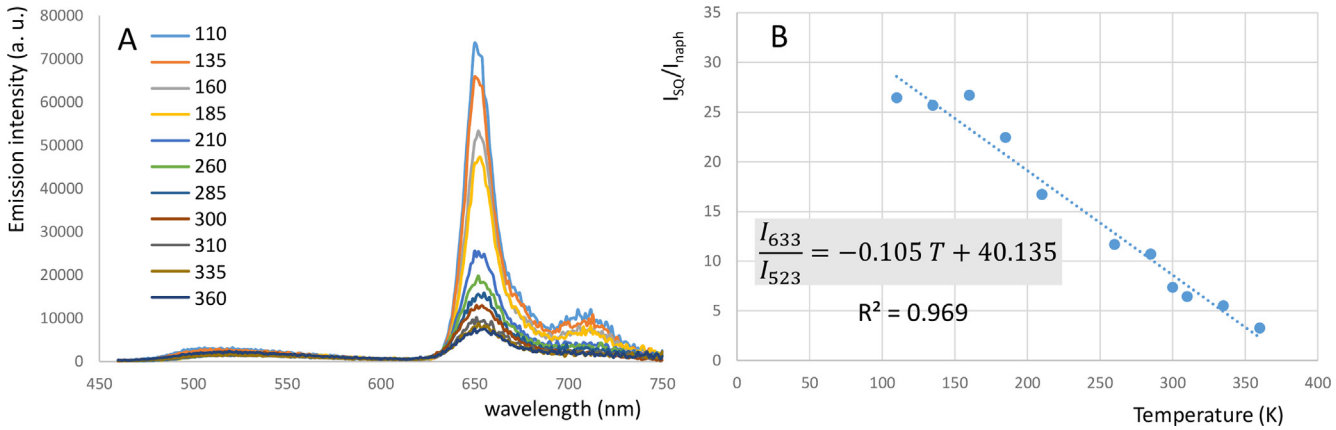

Fig. 5. A) Temperature dependent fluorescence emission spectra and (B) emission intensity ratio (3.2×10^{-6} M, λ_{exc} = 440 nm) of triad **1**.

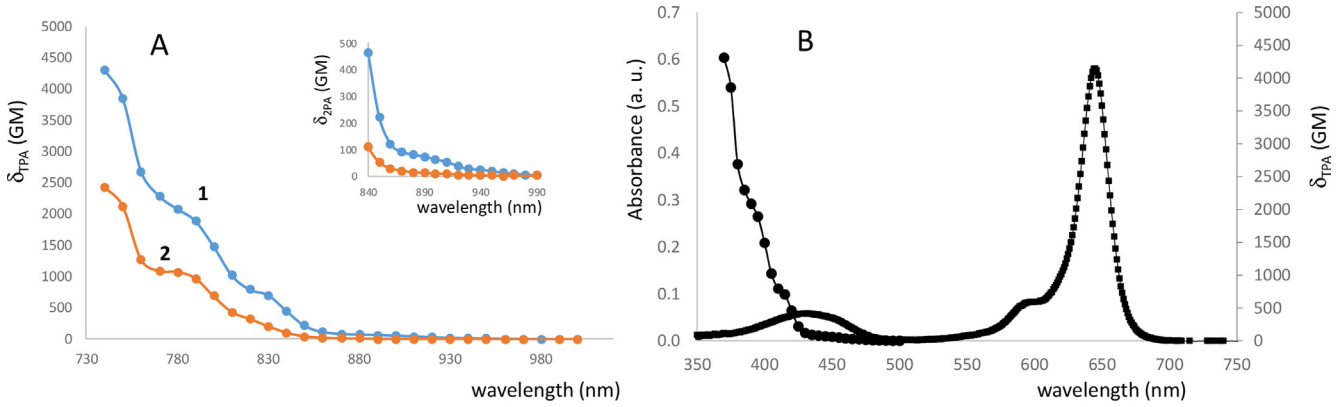

Fig. 6. A) Calculated TPA spectra for **1** and **2** in toluene; B) OPA and TPA spectra for **1** in toluene.

viously looked into by Z-scan measurements, TPET method and quantum-chemical calculations.[36,44] Both fluorophores **1** and **2** show the same TPA bands although in system **1** it is possible to observe the effect of 4-aminoaphthalimide on δ_{TPA} values. The highest intensity TPA band for **1** is observed at 730 nm with $\delta_{TPA} \approx$ 4500 GM. The maximum of this band is not visible due of the tailing of the OPA band. It is crucial to take into account that the TPA cross-section for **2** dips to very small values (2–5 GM) in region between 860 and 1000 nm. For **1**, a band is observed in this region with δ_{TPA} of 81 GM at 880 nm. According to the TPA spectrum of **3**, this band can be easily assigned to a TPA band of 4-aminonaphthalimide with a maximum at 860 nm in toluene (Figure S8). This assumption is confirmed when we compare the TPA and OPA spectra of **1** (Fig. 3.b), as the wavelength shift is in agreement with the main absorption band of naphthalimide. Lastly, the compound **1** combines the TPA features of both chromophores **2** and **3**, what guides to increased TPA cross-sections at 880 nm.

The excitation of **1** under one- (λ_{exc} = 440 nm) and two-photon excitation (λ_{exc} = 880 nm) conditions yields similar λ_{max} in emission spectra in all solvents studied. However, the ratio I_{SQ}/I_{naph} found in TPEF was very different especially in toluene and CH_3CN (Table 3). In the nonpolar solvent toluene, the ratio I_{SQ}/I_{naph} increases significantly (10 times), being favored by low two-photon emissions from naphthalimide.

3.3. Cell imaging

The practical applicability of this highly fluorescent probe was tested with N13 mouse microglial cells. Compound **1** was incubated with the cells in H_2O/DMSO (0.1 vol%) for 1 h at 37 °C. Biological environment is complex within cells, a fluorophore can interact with a multitude of different biomolecules. As we have seen compound **1** exhibits limited interaction via the naphthalimide moiety with proteins. Since the apolar structure of triad **1** it is to be expected that the interaction will be with apolar molecules. Fig. 7.a reveals laser scanning confocal fluorescence microscopy images when direct excitation of the naphthalimide chromophore (λ_{exc} = 458 nm, one-photon excitation conditions) of N13 cells that were incubated with **1**. As it is observed, compound **1** is well internalized by the cells and no proof of morphological damage are detected. When analyzing the images in more detailed, compound **1** appears to be accumulated in the cytoplasm and does not penetrate the cell nucleus that is well delimited.

The samples were lighted up at wavelengths where the naphthalimide absorbs predominantly (λ_{exc} = 458 nm) and the obtained fluorescence corresponded to squaraine (λ_{exc} = 655 nm). The ratio I_{SQ}/I_{naph} was found to be close to 12 inside the cells (Fig. 7.a). This value is very similar to that found in THF which may suggest that the surrounding environment to **1** in cells is similar to that found in THF solution. Comparison of the TPE spectra in cells and in THF solution shows that they are very similar (Figure S10). This result is in agreement with the confocal images that show the fluorophore located principally in bilipid membranes such as the nucleus and other cell vesicles.

N13 cells were also incubated with the compound **1** at a concentration of 5 μM without the washing step and imaged at different times. Even after 10 h of incubation, the fluorophore displayed bright fluorescence in cells with no background fluorescence. Com-

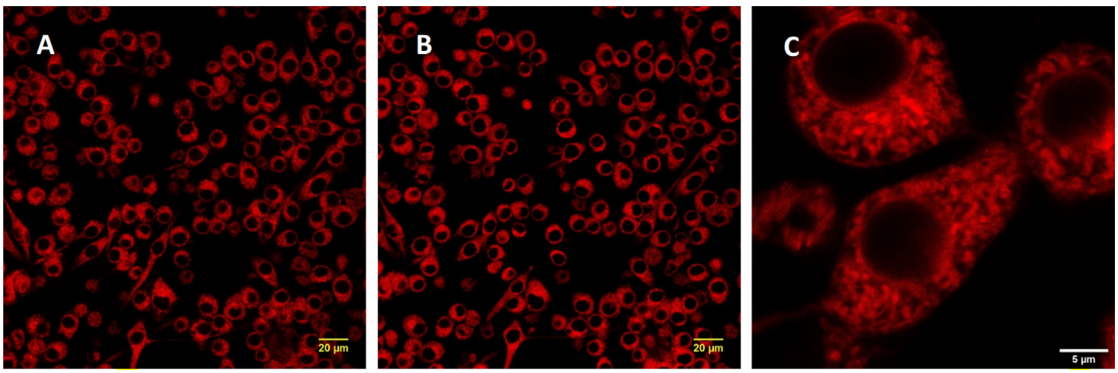

Fig. 7. A) Laser scanning confocal microscopic images of N13 cells incubated for 1 h with **1** (λ_{exc} = 458 nm); B) Two-photon confocal microscopic images of N13 cells incubated **1** (λ_{exc} = 880 nm); C) a magnified image of one cell.

Table 3
TPA cross-section and ratio I_{SQ}/I_{naph} for **1** in some solvents at 880 nm (TPEF) and 440 nm (OPEF).

Solvent	δ_{TPA}	I_{SQ}/I_{naph} TPEF	I_{SQ}/I_{naph} OPEF
TOL	80	130.7	14.9
THF	48	88.5	11.2
$CHCl_3$	15	3.1	8.2
DMF	21	2.4	6.1
CH_3CN	52	0.5	2.4
MeOH	62	3.9	2.0

pound **1** is internalized rapidly inside the cells (even more than at the beginning of the fluorescence measurements). The fluorescence signal reaches its maximum at 45–50 min, with an increase of more than ten times the initial value (figure S11).

The possibility of two-photon excitation below conditions of cell imaging was illustrated with the N13-cell-incubated fluorophore (Fig. 8), yielding closer results when for one-photon excitation conditions. The ratio I_{SQ}/I_{naph} was found to be very high (close to 94) according to what was observed in solution. In Fig. 8.b, it can be seen the emission spectra of chosen points of the confocal microscopic image upon TPE are shown. Since the δ_{TPA} value of **1** was found to be very high, the TPEF microscopy images were very bright, suggesting the potential of this squaraine dye for other bioimaging applications subject to of future investigations.

4. Conclusion

In summary, a new red emissive aminonaphthalimide-squaraine non-conjugated system was synthesized and characterized. The energy transfer between the two fluorophores was found not complete, observing the emission of naphthalimide and squaraine in all the solvents studied. The ratio of these two emissions (I_{SQ}/I_{naph}) has been found to depend on the polarity of the medium. The solvent polarity parameter ET(30) establishes a good correlation between this fluorescence intensity ratio and the polarity of the solvent. The temperature sensing behavior of the triad was evaluated by fluorescence emission in the 110–360 K temperature range. A good correlation was found between the ratio I_{SQ}/I_{naph} with a negative temperature coefficient (-0.105 K^{-1}). The TPEF properties of **1** were studied in different solvent and compared to OPEF. The ratio I_{SQ}/I_{naph} was found higher under two-photon excitation conditions (10-times in toluene). This difference is attributed to the difference in two-photon absorption of squaraine and naphthalimide subchromophores which is much larger for the squaraine fluorophore. The maximum TPA absorption of **1** occurred at 750 nm with δ_{TPA} > 4000 GM. This high value of TPA cross section allows intense fluorescent response signal in TPF microscopy images. Furthermore, stained N13 cells of positive quality images with **1** can be obtained at 880 nm under two photon absorption regime but also at 440 nm upon excitation of naphthalimide chromophore.

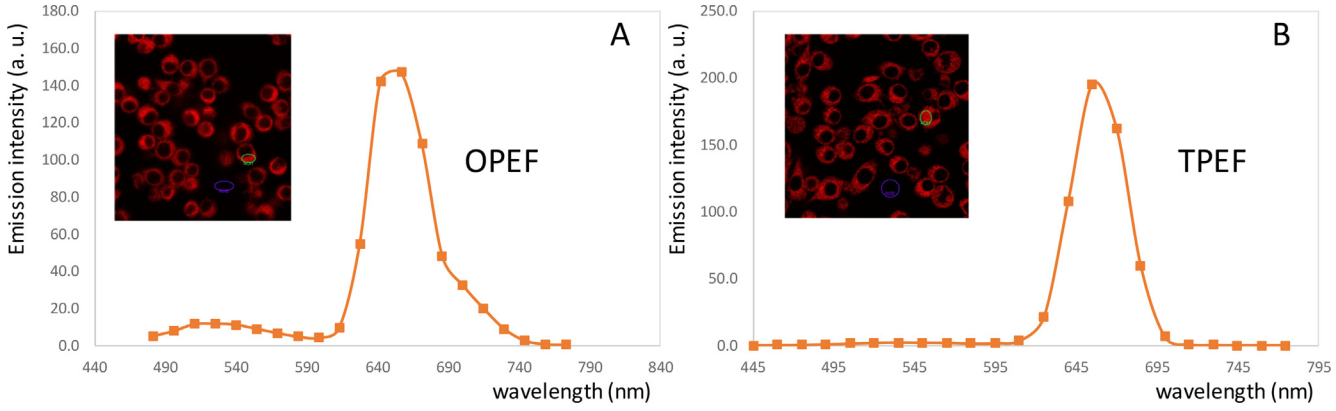

Fig. 8. OPEF (A) and TPEF (B) emission spectra of selected points (ROIs) of N13 cells incubated with **1** upon excitation at 458 and 880 nm.

CRediT authorship contribution statement

Vladimir Stamentović: Conceptualization, Methodology, Investigation, Software, Data curation, Validation, Formal analysis. **Daniel Collado:** Supervision, Investigation, Formal analysis, Writing – review & editing. **Ezequiel Perez-Inestrosa:** Supervision, Resources, Funding acquisition, Investigation, Writing – review & editing.

Declaration of Competing Interest

The authors declare that they have no known competing financial interests or personal relationships that could have appeared to influence the work reported in this paper.

Acknowledgements

This work has been financially supported by MINECO PID2019-104293GB-I00; by Universidad de Málaga-Junta de Andalucía (UMA18-FEDERJA-007), the European Regional Development Fund (ERDF) and "Plan Propio Universidad de Málaga" (UMA-Andalucía-TECH). European Union's Horizon 2020 research and innovation programme under EuroNanoMed 3-H2020 DrNanoDAII and MINECO, PROGRAMACION CONJUNTA 2019/PCI 2019-2. The TPA characterization of compounds has been performed by the ICTS "NANBIOSIS", more specifically by the U28 Unit of the Andalusian Centre for Nanomedicine & Biotechnology (BIONAND) . This project has received funding from the European Union's Horizon 2020 research and innovation programme under the Marie Skłodowska-Curie grant agreement No. 713721.

Appendix A. Supplementary data

Supplementary data to this article can be found online at https://doi.org/10.1016/j.saa.2021.120546.

References

[1] S. Shah, W. Mandecki, J. Li, Z. Gryczynski, J. Borejdo, I. Gryczynski, R. Fudala, FRET study in oligopeptide-linked donor–acceptor system in PVA matrix, Methods Appl. Fluoresc. 4 (2016), https://doi.org/10.1088/2050-6120/4/4/047002 047002.
[2] B. Wallace, P.J. Atzberger, Förster resonance energy transfer: Role of diffusion of fluorophore orientation and separation in observed shifts of FRET efficiency, PLoSONE 12 (5) (2017), https://doi.org/10.1371/journal.pone.0177122 e0177122.
[3] J. Fan, M. Hu, P. Zhana, X. Peng, Energy transfer cassettes based on organic fluorophores: construction and applications in ratiometric sensing, Chem. Soc. Rev. 42 (2013) 29–43, https://doi.org/10.1039/C2CS35273G.
[4] P. Horváth, P. Šebej, T. Šolomek, P. Klán, Small-molecule fluorophores with large stokes shifts: 9-iminopyronin analogues as clickable tags, J. Org. Chem. 80 (2015) 1299–1311, https://doi.org/10.1021/jo502213t.
[5] G.-S. Jiao, A. Loudet, H.B. Lee, S. Kalinin, L.-B.-A. Johansson, K. Burgess, Syntheses and spectroscopic properties of energy transfer systems based on squaraines, Tetrahedron 59 (2003) 3109–3116, https://doi.org/10.1016/S0040-4020(03)00383-1.
[6] D. Collado, P. Remón, Y. Vida, F. Najera, P. Sen, U. Pischel, E. Perez-Inestrosa, Energy Transfer in Aminonaphthalimide-Boron-Dipyrromethene (BODIPY) Dyads upon One- and Two-Photon Excitation: Applications for Cellular Imaging, Chem. Eur. J. 9 (2014) 797–804, https://doi.org/10.1002/asia.201301334.
[7] J.O. Escobedo, O. Rusin, S. Lim, R.M. Strongin, NIR dyes for bioimaging applications, Curr. Opin. Chem. Biol. 14 (1) (2010) 64–70, https://doi.org/10.1016/j.cbpa.2009.10.022.
[8] W. Sun, S. Guo, C. Hu, J. Fan, X. Peng, Recent Development of Chemosensors Based on Cyanine Platforms, Chem. Rev. 116 (2016) 7768–7817, https://doi.org/10.1021/acs.chemrev.6b00001.
[9] S. Yagi, H. Nakazumi, in: Topics in Heterocyclic ChemistryHeterocyclic Polymethine Dyes, Springer Berlin Heidelberg, Berlin, Heidelberg, 2008, pp. 133–181.
[10] H.M. Kim, B.R. Cho, Small-Molecule Two-Photon Probes for Bioimaging Applications, Chem. Rev. 115 (11) (2015) 5014–5055, https://doi.org/10.1021/cr5004425.
[11] S. Yao, K.D. Belfield, Two-photon fluorescent probes for bioimaging, Eur. J. Org Chem. 2012 (17) (2012) 3199–3217, https://doi.org/10.1002/ejoc.v2012.1710.1002/ejoc.201200281.
[12] T.D. Martins, M.L. Pacheco, R.E. Boto, P. Almeida, J.P.S. Farinha, L.V. Reis, Synthesis, characterization and protein-association of dicyanomethylene squaraine dyes, Dyes Pigm. 147 (2017) 120–129, https://doi.org/10.1016/j.dyepig.2017.07.070.
[13] a) I.V. Hovor, O.S. Kilosova, E.V. Sanin, O.M. Obukhova, A.L. Tatarets, E.A. Terpetshihig, L.D. Patsenker, Water-soluble norsquaraine dyes for protein labeling and pH-sensing applications, Dyes Pigm. 170 (2019), https://doi.org/10.1016/j.dyepig.2019.107567 107567.
[14] S.-L. Sun, S.-K. Lv, Y.-P. Liu, Q. Liao, H.-L. Zhang, H. Fu, S.J. Yao, Benzoindolic squaraine dyes with a large two-photon absorption cross-section, J. Mater. Chem. C 5 (2017) 1224–1230, https://doi.org/10.1364/oe.27.012360.
[15] R.M. Duke, E.B. Veale, F.M. Pfeffer, P.E. Kruger, T. Gunnlaugsson, Colorimetric and fluorescent anion sensors: An overview of recent developments in the use of 1,8-naphthalimide-based chemosensors, Chem. Soc. Rev. 39 (2010) 3936–3953, https://doi.org/10.1039/B910560N.
[16] H. Yao, Advanced Fluorescence Reporters in Chemistry and Biology II. Advanced Fluorescence Reporters in Chemistry and Biology II Vol. 9 (2010) 66–104.
[17] A. Saini, K.R. Justin Thomas, A. Sachdev, P. Gopinath, Photophysics, electrochemistry, morphology, and bioimaging applications of new 1,8-naphthalimide derivatives containing different chromophores, Chem. Eur. J. 12 (2017) 2612–2622, https://doi.org/10.1002/asia.201700968.
[18] W.V. Moreshead, O.V. Przhonska, M.V. Bondar, A.D. Kachkovski, I.H. Nayyar, A. E. Masunov, A.W. Woodward, K.D. Belfield, Design of a new optical material with broad spectrum linear and two-photon absorption and solvatochromism, J. Phys. Chem. C 117 (44) (2013) 23133–23147, https://doi.org/10.1021/jp406500t.
[19] S. de Reguardati, J. Pahapill, A. Mikhailov, Y. Stepanenko, A. Rebane, High-accuracy reference standards for two-photon absorption in the 680–1050 nm wavelength range, Opt. Express 24 (2016) 9053–9066, https://doi.org/10.1364/OE.24.009053.
[20] M. Rumi, J.W. Perry, Two-photon absorption: an overview of measurements and principles, Adv. *Opt. Photonics* 2 (2010) 451–518, https://doi.org/10.1364/AOP.2.000451.
[21] S. Khopkar, S. Deshpande, G. Shankarling, Greener Protocol for the Synthesis of NIR Fluorescent Indolenine-Based Symmetrical Squaraine Colorants, ACS Sustain. Chem. Eng. 6 (8) (2018) 10798–10805, https://doi.org/10.1021/acssuschemeng.8b02095.
[22] I.A. Karpenko, A.S. Klymchenko, S. Gioria, R. Kreder, I. Shulov, P. Villa, Y. Mély, M. Hibert, D. Bonnet, Squaraine as a bright, stable and environment-sensitive far-red label for receptor-specific cellular imaging, Chem. Commun. 51 (14) (2015) 2960–2963, https://doi.org/10.1039/C4CC09113B.
[23] C. Laia, S. Costa, Ground- and excited-state solvation of a squaraine dye by water in dioxane, Chem. Phys. Lett. 285 (1998) 385–390, https://doi.org/10.1021/jp406500t.
[24] E. Terpetschnig, H. Szmacinski, J.R. Lakowicz, Synthesis, spectral properties and photostabilities of symmetrical and unsymmetrical squaraines; a new class of fluorophores with long-wavelength excitation and emission, Anal. Chim. Acta 282 (1993) 633–641, https://doi.org/10.1021/jp406500t.
[25] N.I. Georgiev, V.B. Bojinov, P.S. Nikolov, Design and synthesis of a novel pH sensitive core and peripherally 1,8-naphthalimide-labeled PAMAM dendron as light harvesting antenna, Dyes Pigm. 81 (1) (2009) 18–26, https://doi.org/10.1016/j.dyepig.2008.08.009.
[26] J.R. Lakowicz, Principles of Fluorescence Spectroscopy, 3rd ed.;., Kluwer Academic/Plenum Publishers:, 2007.
[27] A.R. Ballestas-Barrientos, A.W. Woodward, W.V. Moreshead, M.V. Bondar, K.D. Belfield, Synthesis and linear and nonlinear photophysical characterization of two symmetrical pyrene-terminated squaraine derivatives, J. Phys. Chem. C 120 (14) (2016) 7829–7838, https://doi.org/10.1021/acs.jpcc.6b0014310.1021/acs.jpcc.6b00143.s001.
[28] A.S. Tatikolov, Sílvia.M.B. Costa, Photophysical and aggregation properties of a long-chain squarylium indocyanine dye, J. Photochem. Photobiol. A: Chem. 140 (2) (2001) 147–156, https://doi.org/10.1016/S1010-6030(01)00405-1.
[29] J.P. Cerón-Carrasco, D. Jacquemin, C. Laurence, A. Planchat, C. Reichardt, K. Sraïdi, Solvent polarity scales: determination of new ET(30) values for 84 organic solvents, J. Phys. Org. Chem. 27 (6) (2014) 512–518, https://doi.org/10.1002/poc.v27.610.1002/poc.3293.
[30] A.C. Benniston, A. Harriman, V.L. Whittle, M. Zelzer, Molecular rotors based on the boron dipyrromethene fluorophore, European J. Org. Chem. 2010 (3) (2010) 523–530, https://doi.org/10.1002/ejoc.v2010:310.1002/ejoc.200901135.
[31] C. Laia, S. Costa, Fluorescence quenching of a squaraine dye by water in AOT reversed micelles, J. Chem. Soc., Faraday Trans. 94 (1998) 2367–2373, https://doi.org/10.1039/A802740D.
[32] A.L. Tatarets, I.A. Fedyunyayeva, T.S. Dyubko, Y.A. Povrozin, A.O. Doroshenko, E. A. Terpetschnig, L.D. Patsenker, Synthesis of water-soluble, ring-substituted squaraine dyes and their evaluation as fluorescent probes and labels, Anal. Chim. Acta 570 (2006) 214–223, https://doi.org/10.1021/am300467w.

[33] Y. Zhang, X. Yue, B. Kim, S. Yao, K.D. Belfield, Deoxyribonucleoside-modified squaraines as near-IR viscosity sensors, Chem. Eur. J. 20 (24) (2014) 7249–7253, https://doi.org/10.1002/chem.201403003.
[34] E.J. McLaurin, A.B. Greytak, M.G. Bawendi, D.G. Nocera, Two-Photon Absorbing Nanocrystal Sensors for Ratiometric Detection of Oxygen, J. Am. Chem. Soc. 131 (36) (2009) 12994–13001, https://doi.org/10.1021/ja902712b.
[35] J.J. McEwen, K.J. Wallace, Squaraine dyes in molecular recognition and self-assembly, Chem. Commun. (42) (2009) 6339, https://doi.org/10.1039/b909572a.
[36] R. Yi, P. Das, F. Lin, B. Shen, Z. Yang, Y. Zhao, L. Hong, Y. He, R. Hu, J. Song, J. Qu, L. Liu, Fluorescence enhancement of small squaraine dye and its two-photon excited fluorescence in long-term near-infrared I&II bioimaging, Opt. Express 27 (2019) 12360, https://doi.org/10.1364/oe.27.012360.
[37] I.V. Hovor, O.S. Kolosova, E.V. Sanin, O.M. Obukhova, A.L. Tatarets, E.A. Terpetschnig, L.D. Patsenker, Water-soluble norsquaraine dyes for protein labeling and pH-sensing applications, Dye. Pigment. 170 (2019) 107567, https://doi.org/10.1016/j.dyepig.2019.107567.
[38] K. Rani, U.K. Pandey, S. Sengupta, Efficient electron transporting and panchromatic absorbing FRET cassettes based on aza-BODIPY and perylenediimide towards multiple metal FRET-Off sensing and ratiometric temperature sensing, J. Mater. Chem. C. 9 (13) (2021) 4607–4618, https://doi.org/10.1039/D1TC00068C.
[39] K.-Y. Law, Squaraine chemistry: effects of solvent and temperature on the fluorescence emission of squaraines, J. Photochem. Photobiol. A: Chem. 84 (2) (1994) 123–132, https://doi.org/10.1016/1010-6030(94)03849-X.
[40] T. Terai, T. Nagano, Small-molecule fluorophores and fluorescent probes for bioimaging, *Pflugers Arch. Eur*, J. Physiol. 465 (3) (2013) 347–359, https://doi.org/10.1007/s00424-013-1234-z.
[41] F. Terenziani, C. Katan, E. Badaeva, S. Tretiak, M. Blanchard-Desce, Enhanced two-photon absorption of organic chromophores: Theoretical and experimental assessments, Adv. Mat. 20 (24) (2008) 4641–4678, https://doi.org/10.1002/adma.v20:2410.1002/adma.200800402.
[42] V. Grande, C.-A. Shen, M. Deiana, M. Dudek, J. Olesiak-Banska, K. Matczyszyn, F. Würthner, Selective parallel G-quadruplex recognition by a NIR-to-NIR two-photon squaraine, Chem. Sci. 9 (44) (2018) 8375–8381, https://doi.org/10.1039/C8SC02882F.
[43] S. Webster, S.A. Odom, L.A. Padilha, O.V. Przhonska, D. Peceli, H. Hu, G. Nootz, A.D. Kachkovski, J. Matichak, S. Barlow, H.L. Anderson, S.R. Marder, D.J. Hagan, E.W. Van Stryland, Linear and nonlinear spectroscopy of a porphyrin-squaraine-porphyrin conjugated system, J. Phys. Chem. B 113 (45) (2009) 14854–14867, https://doi.org/10.1021/jp904460f.
[44] J. Fu, L.A. Padilha, D.J. Hagan, E.W. Van Stryland, O.V. Przhonska, M.V. Bondar, Y.L. Slominsky, A.D. Kachkovski, Experimental and theoretical approaches to understanding two-photon absorption spectra in polymethine and squaraine molecules, J. Opt. Soc. Am. B 24 (2007) 67–76, https://doi.org/10.1364/JOSAB.24.000067.